

PAPER

A phenomenological model for interfacial water near hydrophilic polymers

To cite this article: A Earls *et al* 2022 *J. Phys.: Condens. Matter* **34** 355102

View the [article online](#) for updates and enhancements.

You may also like

- [The amorphous silica-liquid water interface studied by *ab initio* molecular dynamics \(AIMD\): local organization in global disorder](#)
Álvaro Cimas, Frederik Tielens, Marialore Sulpizi *et al.*

- [Coexistence of slow and fast dynamics in interfacial water around a carbon nanotube](#)
Yusei Kioka, Takemi Hara, Yuki Maekawa *et al.*

- [Oxide/water interfaces: how the surface chemistry modifies interfacial water properties](#)
Marie-Pierre Gaigeot, Michiel Sprak and Marialore Sulpizi

A phenomenological model for interfacial water near hydrophilic polymers

A Earls^{1,*} , M-C Calderer² , M Desroches³ , A Zarnescu^{1,4,5}  and S Rodrigues^{1,4,*} 

¹ Basque Center for Applied Mathematics, Bilbao, Spain

² University of Minnesota, Minneapolis, MN, United States of America

³ Inria at Université Côte d'Azur, Sophia Antipolis, France

⁴ Ikerbasque, Bilbao, Spain

⁵ Simion Stoilow Institute of the Romanian Academy, Bucharest, Romania

E-mail: aearls@bcamath.org and srodrigues@bcamath.org

Received 5 April 2022, revised 25 May 2022

Accepted for publication 22 June 2022

Published 30 June 2022



Abstract

We propose a minimalist phenomenological model for the ‘interfacial water’ phenomenon that occurs near hydrophilic polymeric surfaces. We achieve this by combining a Ginzburg–Landau approach with Maxwell’s equations which leads us to a well-posed model providing a macroscopic interpretation of experimental observations. From the derived governing equations, we estimate the unknown parameters using experimental measurements from the literature. The resulting profiles of the polarization and electric potential show exponential decay near the surface, in qualitative agreement with experiments. Furthermore, the model’s quantitative prediction of the electric potential at the hydrophilic surface is in excellent agreement with experiments. The proposed model is a first step towards a more complete parsimonious macroscopic model that will, for example, help to elucidate the effects of interfacial water on cells (e.g. neuronal excitability), the effects of infrared neural stimulation or the effects of drugs mediated by interfacial water.

Keywords: interfacial water, exclusion zone, hydrophilic polymers

1. Introduction

Water is an ubiquitous material and intrinsically associated with life. Its anomalous behavior is recognized as the origin of various phenomena in chemistry and biology. One such anomalous behavior occurs when liquid water interacts with hydrophilic polymeric surfaces (e.g. cellular membranes). These are interfaces of polymeric materials which have high affinity with water. At a microscopic scale it has been seen that the hydrophilic surface affects the electric polarization of water layers. However the mechanism for generating this polarization, based on the deformation of water molecules, is not well

understood. The current paper only aims to provide a phenomenological description of this phenomenon.

Near the hydrophilic surfaces a specific phase of water was observed. This is called ‘interfacial water’ and has emergent physical-chemical properties (different from usual liquid state of water), such as, non-zero electrical potential, reacts to light [1] and repels materials (e.g. solutes [2]). The width of the interfacial layer varies, but can range from hundreds of microns to several millimeters [3, 4]. The interfacial layer is typically negatively charged (but there are exceptions [5]), and the electric potential at the hydrophilic surface is negative. The layer causes charge separation in the fluid, creating a ‘nanobattery’, and therefore it may have an important role in biology [6, 7]. However, despite the accumulation of a vast body of experimental evidence and theoretical approaches, the exact

* Authors to whom any correspondence should be addressed.

mechanisms that causes the emergence of interfacial layer is still being debated. As yet there is no macroscopic, well-posed mathematical model able to describe and predict properties of the interfacial layer. A first step is proposed in the present work.

The proposed explanations for the formation of the interfacial layer include diffusiophoresis and ion exchange [3, 8, 9], repulsive van der Waals forces [10], or a new phase of water which is fundamentally different than the bulk one [11].

In this paper, we aim to produce a minimalistic mathematical model that predicts the interfacial water phenomenon but does not assume any particular physical mechanism is responsible for the interfacial layer formation. In section 2, we present the derivation of the model. As a first approach, we neglect ionic charges and take the unknowns of the problem to be the polarization p and the electric potential Φ . For simplicity, we will consider a one-dimensional region of water, $0 < z < M$, with a hydrophilic surface located at $z = 0$.

To obtain the governing equations for the system, we focus on the long-time regime in which the system is stationary, postulate an energy density $\mathcal{E}(p, p', \Phi')$ and apply a variational method. Several parameters in the energy density \mathcal{E} are phenomenological and must be estimated. In section 3, we first study a simplified system with an infinite domain ($M = +\infty$) and constant relative permittivity throughout the interfacial region. In this scenario the Euler–Lagrange (EL) equations admit an exact solution, and we use experimental measurements from the literature to reverse engineer and estimate the necessary quantities.

With these parameter estimates in hand, in section 4 we then study the problem on a finite domain, $M < \infty$. We also allow the relative permittivity to vary throughout the interfacial region by writing it as a function of z , the distance from the hydrophilic surface. In each scenario, we find that the polarization and potential profiles have qualitatively the same shape. Also, both approaches give excellent estimates of the electric potential at the surface.

2. Modeling framework

In this section, we define the energy and pose the EL equations on both domain types.

Far away from the hydrophilic surface, the water should be in its usual nonpolar phase:

$$p(z = M) = 0 \text{ C m}^{-2}, \quad \Phi'(z = M) = 0 \text{ V m}^{-1}. \quad (1)$$

At the surface, the water should be polarized:

$$p(z = 0) = p_0. \quad (2)$$

We will also assume:

$$\Phi(M) = 0 \text{ V}. \quad (3)$$

The electric displacement is defined as $D = \varepsilon_0 \varepsilon(z) E + p$, so the electric energy density is expressed as:

$$\mathcal{E}_{\text{elec}} = - \int D \, dE = -\frac{1}{2} \varepsilon_0 \varepsilon(z) (\Phi')^2 + p \Phi'. \quad (4)$$

We also define a double-well Ginzburg–Landau potential for the polarization, with potential wells of depth quantified by the constant δ :

$$\mathcal{E}_{\text{GL}}(p) = \frac{p^2}{2\delta^2} (p - ap_0)^2. \quad (5)$$

The energy density \mathcal{E}_{GL} encodes the fact that the fluid has two preferred states: nonpolar ($p = 0$), or polarized ($p = ap_0$). The constant a is one of the phenomenological parameters to be determined. The states $p = 0$ and $p = ap_0$ represent the bulk water phase and the interfacial phase, respectively. The solution we seek will exhibit a transition between these two states.

We then model the solution (p, Φ) as a critical point of the following energy functional:

$$E[p, \Phi] = \int_0^M \mathcal{E}(p, p', \Phi') \, dz, \quad (6)$$

$$\mathcal{E}(p, p', \Phi') = \frac{1}{2} \kappa(p')^2 + \mathcal{E}_{\text{GL}}(p) + \mathcal{E}_{\text{elec}}(p, \Phi'). \quad (7)$$

The three terms of the energy density \mathcal{E} model the spatial variations of p , the phase transition, and the interaction between p and Φ , respectively. We seek a critical point (p, Φ) of (7) that satisfies the boundary conditions (1) and (3).

Hence, applying the principle of least action to the energy (7) yields the EL equations:

$$\left(\frac{\partial \mathcal{E}}{\partial p'} \right)' - \frac{\partial \mathcal{E}}{\partial p} = 0, \quad (8)$$

$$\left(\frac{\partial \mathcal{E}}{\partial \Phi'} \right)' - \frac{\partial \mathcal{E}}{\partial \Phi} = 0. \quad (9)$$

Equation (9) is Poisson's equation, which reduces to:

$$(\varepsilon_0 \varepsilon(z) \Phi')' = p', \quad (10)$$

and can be integrated to give:

$$\Phi' = \frac{p}{\varepsilon_0 \varepsilon(z)}. \quad (11)$$

Equation (8) can then be written:

$$\kappa p'' = p \left[\frac{1}{\delta^2} (p - ap_0)(2p - ap_0) + \frac{1}{\varepsilon_0 \varepsilon(z)} \right]. \quad (12)$$

Note that $p = 0$ is an equilibrium point of (12), corresponding to the nonpolar water state. In the next two sections, we will solve (11) and (12), subject to the boundary conditions (1)–(3).

3. Parameter estimation

We first study the problem with some simplifications in order to estimate the unknown parameters a , p_0 , κ , and δ^2 . First, we assume that the sample size is much larger than the width of the interfacial layer and set $M = +\infty$ so that the domain is infinite. Next, assume that the dielectric permittivity is constant

throughout the interfacial layer: $\varepsilon(z) = \varepsilon_W$, where $\varepsilon_W = 80$ is the bulk value. Recent experiments show that within a few nanometers of the hydrophilic surface, the permittivity drops to about $\varepsilon_{\text{int}} = 2$ [12]. On the other hand, we expect the interfacial layer to be several hundred microns wide. Because of this difference in length scales, it is reasonable to assume in this initial approach that $\varepsilon(z) = \text{const}$.

The exact solution in this case is (see the [appendix](#) for the calculation):

$$p(z) = \frac{p_0 \sqrt{\lambda}(\beta^2 + 1)}{\beta + \sinh \omega}, \quad (13)$$

$$\Phi(z) = \frac{2\sqrt{\kappa\delta^2}}{\varepsilon_0\varepsilon_W} \left[\tanh^{-1} \left(\frac{\beta \tanh(\omega/2) - 1}{\sqrt{\beta^2 + 1}} \right) - \tanh^{-1} \left(\frac{\beta - 1}{\sqrt{\beta^2 + 1}} \right) \right], \quad (14)$$

with

$$\omega(z; a, \lambda) = \sqrt{\frac{\beta^2 + 1}{\varepsilon_0\varepsilon_W\kappa}} z + c, \quad (15)$$

$$\lambda = \frac{\delta^2}{\varepsilon_0\varepsilon_W p_0^2}, \quad (16)$$

$$\beta(a, \lambda) = \frac{a}{\sqrt{\lambda}}, \quad (17)$$

$$c(a, \lambda) = \tanh^{-1} \left(\frac{a^2 - a + \lambda}{\sqrt{a^2 + \lambda} \sqrt{(a - 1)^2 + \lambda}} \right). \quad (18)$$

The goal of this section is to estimate the unknown quantities p_0 , a , δ^2 , and κ which determine the solution (14)–(18).

Equation (11) implies $p_0 = -E_0/(\varepsilon_0\varepsilon_W)$, where E_0 is the electric field at the hydrophilic surface. We can therefore estimate p_0 using the value $E_0 = -40 \text{ mV}^{-1}$ [9, figure 4(c)].

To estimate the remaining parameters, we make several assumptions. First, we suppose that the boundary condition $p = p_0$ is a stationary solution to (12). In this case p' is approximately constant near the hydrophilic surface at $z = 0$. This assumption gives $\lambda = \lambda(a)$.

Next, observe that both $p(z)$ and $\Phi(z)$ depend on z only through the function $\omega(z; a, \lambda)$ defined in (18). The length scale of the solution is determined by β , and we select a so that $\beta(a, \lambda(a))$ gives the largest possible length scale. This will give the largest interfacial layer in the solution.

Finally, it remains to estimate the parameter κ . Observe that $p'' = 0$ at $z = 0$ (from the first assumption) and at $z = +\infty$, where $p = 0$. Between these two endpoints, p'' has a maximum, say at z_0 . Roughly speaking, for $z < z_0$ (near the hydrophilic surface), the polarization profile $p(z)$ resembles an exponentially decaying function, and for $z > z_0$, $p(z)$ begins to level out. The point $z = z_0$ can then be understood as the boundary between the interfacial layer and the rest of the cell. In order to

estimate κ , we will now first approximate $z_0 = L_{\text{IF}}$, where L_{IF} is an experimental measurement of the interfacial layer thickness, and then work backwards.

There are many measurements of the interfacial layer thickness in the literature [3, 4, 9, 13–15]. Florea *et al* [3] find that the layer width grows with time, up to a few millimeters. Since our model is stationary, the solution (p, Φ) in (14) represents the eventual, long-time state, and we expect the layer width to be large. We therefore approximate $L_{\text{IF}} = 2 \text{ mm}$.

With the above assumptions, we obtain the following parameter estimates:

$$p_0 = 2.8 \times 10^{-8} \text{ C m}^{-2} \quad (19)$$

$$\delta^2 = 10^{-25} \text{ m}^2 \text{ N}^{-1}, \quad (20)$$

$$a = \frac{4}{3}, \quad (21)$$

$$\kappa = 1.5 \times 10^4 \text{ N m}^4 \text{ C}^{-2}. \quad (22)$$

We also find that at the edge of the interfacial layer, the polarization is at one-third of its maximum value. That is, $p(z = L_{\text{IF}}) = p_0/3$. Figure 1 shows the solution (14)–(18) for the parameters (19).

Though we have made several simplifications, this exact solution also provides an excellent prediction of the electric potential at the surface. Experiments show [4, figure 3(a)] that the electric potential at the surface is on the order of -60 mV , and with parameters as above the model predicts $\Phi(0) = -68 \text{ mV}$.

4. With correction to permittivity

We consider again the problem (10)–(12), subject to (1)–(3), without the simplifying assumptions of the previous section. We use the parameter values (19)–(22) and choose the domain size to be $M = 1 \text{ cm}$. Additionally, we allow the permittivity to depend on the distance z from the surface, with:

$$\varepsilon(z) = \varepsilon_{\text{int}} + \frac{\varepsilon_W - \varepsilon_{\text{int}}}{1 + \exp(-\alpha(z - \hat{z}))}. \quad (23)$$

In (23), $\varepsilon_{\text{int}} = 2$ is the value of the permittivity in the interface, and the distance \hat{z} is on the order of a few molecular lengths [16]. The profile of $\varepsilon(z)$ is shown in figure 2(a), with $\hat{z} = 10 \text{ nm}$ and $\alpha = 10^7 \text{ m}^{-1}$.

Comparing figures 1 and 2, we find that the polarization and potential profiles are nearly identical. Therefore, we can conclude *a posteriori* that the approximation $\varepsilon(z) \approx \varepsilon_W$ made in the previous section was reasonable. This is not surprising, since in (23), the region where $\varepsilon \approx \varepsilon_{\text{int}}$ is only about 10 nm wide, orders of magnitude smaller than the width of the interfacial layer.

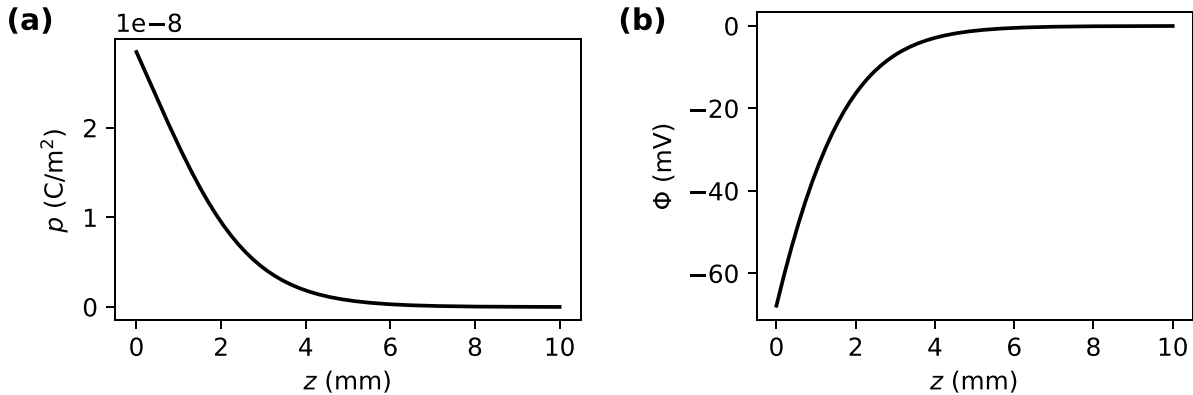


Figure 1. The solution (14)–(18) for the polarization p (a) and the electric potential Φ (b). The polarization and electric potential profiles have the qualitatively the shape that appears in experiments, and the value of the potential at the surface is $\Phi(0) = -68$ mV.

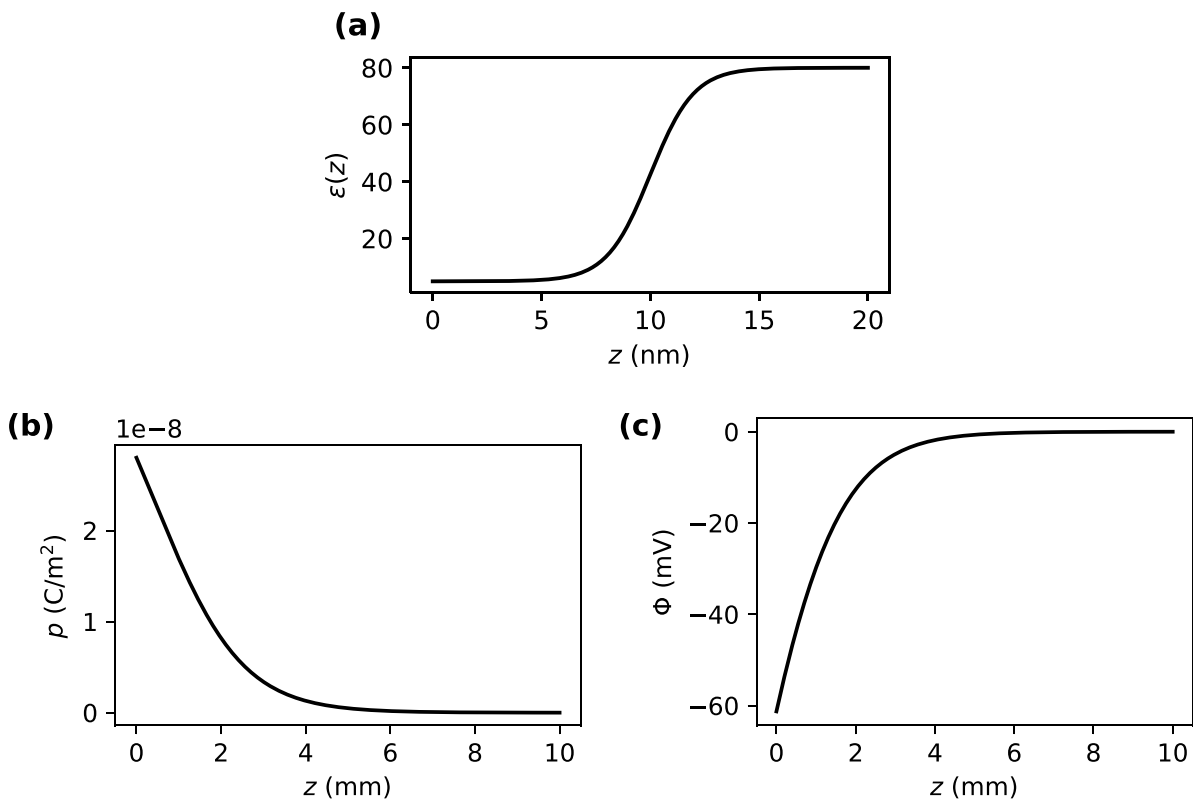


Figure 2. (a). Dielectric permittivity profile defined in (23). (b), (c) Numerical solution for p and Φ , respectively, with $M = 1$ cm, $\varepsilon = \varepsilon(z)$ as in (23), and parameters as in (19). The value of the potential at the surface is $\Phi(0) = -61$ mV.

5. Conclusion

We have developed a simple model for the electric polarization and potential within the interfacial layer of water near a hydrophilic surface. We postulated an energy law with a double-well potential describing the two preferred states of the polarization, derived the governing equations, and studied the solutions in two regimes. First, we studied the problem on an infinite domain, with constant dielectric permittivity, employing experimental measurements of the electric field and the layer thickness in order to estimate the phenomenological parameters which appear in the energy. We then used the

found parameter values to study the same problem on a finite domain, with varying permittivity. The polarization and potential profiles in both regimes are exponentially decaying and show good agreement with experiment. Crucially, our model predicts that the electric potential at the hydrophilic surface is -68 mV for the infinite domain, or -61 mV for the finite domain. Experiment shows [4] that the electric potential at the surface is about -60 mV, matching our model prediction very well.

The proposed model is one-dimensional and neglects ionic effects. This work therefore does not rule out any of the proposed explanations for the formation of the interfacial layer.

In an upcoming work, we will expand the current model to include the possible physical mechanisms responsible for the interfacial water phenomenon.

The present work sets our long term goal to develop a model for understanding the role of interfacial water in biological systems. An important class of such systems are excitable cellular media, such as neuronal cells and heart cells that mediate their functions via electrical-chemical signals. Since interface water exhibits non-neutral potential then it is reasonable to ask whether the standard neuronal models (e.g. Hodgkin–Huxley), which assume neutral water and ions as the main mediators for excitability, are sufficiently correct. A fundamental feature of interfacial water is that it reacts to light (including infrared) by expanding the size of the interfacial layer. Interestingly, recent neuronal experiments have shown that mid-infrared light (by carefully avoiding thermal contributions) increases neuronal excitability, thus hinting at the fact that interfacial water is at play [17]. In this context our model opens a novel avenue of enquiry, which will help clarify if excitable cellular media and in general biological systems exploit the energy in interfacial water to mediate their cellular functions.

Data availability statement

No new data were created or analysed in this study.

Acknowledgments

S R and M D are grateful to Professor Vera Maura Fernandes de Lima for very insightful discussions on interfacial water. S R and A Z acknowledge support from Ikerbasque (The Basque Foundation for Science). A E, S R and A Z acknowledge the support of the Basque Government through the BERC 2018–2021 program and the Spanish State Research Agency through BCAM Severo Ochoa excellence accreditation SEV-2017-0718 and through Project RTI2018-093860-B-C21 funded by (AEI/FEDER, UE) and acronym ‘MathNEURO’. M D and S R acknowledge the support of Inria via the Associated Team ‘NeuroTransSF’. A Z acknowledges the support of Project PID2020-114189RB-I00, acronym ‘LICI’ funded by Agencia Estatal de Investigación (PID2020-114189RB-I00/AEI/10.13039/501100011033).

Appendix

In this appendix, we show the calculations to obtain the solution (14)–(18) and the parameter estimates (19)–(22) presented in section 3. First, we must solve:

$$\kappa p'' = p \left[\frac{1}{\delta^2} (p - ap_0)(2p - ap_0) + \frac{1}{\varepsilon_0 \varepsilon_W} \right], \quad (\text{A.1})$$

$$p(0) = p_0, \quad (\text{A.2})$$

$$p(+\infty) = 0. \quad (\text{A.3})$$

(As in section 3, we have assumed that $M = +\infty$ and $\varepsilon(z) = \varepsilon_W$, with $\varepsilon_W = 80$ denoting the relative permittivity of liquid water.) The solution to (A.1)–(A.3) can be computed analytically.

It is convenient to remove dimension from the equation. Let L be a typical length scale of the system, introduce the dimensionless variables:

$$\bar{z} = \frac{z}{L}, \quad \bar{p}(\bar{z}) = \frac{p(z)}{p_0}. \quad (\text{A.4})$$

and observe that:

$$\frac{\partial}{\partial z} = \frac{1}{L} \frac{\partial}{\partial \bar{z}}. \quad (\text{A.5})$$

With this change of variables, (A.1)–(A.3) become:

$$\mu \bar{p}_{\bar{z}\bar{z}} = \bar{p} [(\bar{p} - a)(2\bar{p} - a) + \lambda], \quad (\text{A.6})$$

$$\bar{p}(0) = 1, \quad (\text{A.7})$$

$$\bar{p}(+\infty) = 0, \quad (\text{A.8})$$

for

$$\mu = \frac{\kappa \delta^2}{p_0^2 L^2}, \quad \lambda = \frac{\delta^2}{\varepsilon_0 \varepsilon_W p_0^2}. \quad (\text{A.9})$$

Multiply (A.6) by $2\bar{p}_{\bar{z}}$ and integrate once to obtain:

$$\mu (\bar{p}_{\bar{z}})^2 = \bar{p}^2 [(\bar{p} - a)^2 + \lambda] + c_1. \quad (\text{A.10})$$

We first assume that we can take the integration constant c_1 to be zero so that $d\bar{p}/d\bar{z} \rightarrow 0$ as $\bar{z} \rightarrow +\infty$; we will later verify that this is the correct choice of c_1 . Then the only constant solution to (A.10) is the nonpolar state $\bar{p} = 0$, and (A.11) can be rewritten:

$$\frac{\bar{p}_{\bar{z}}}{\bar{p}} \left[\left(\frac{\bar{p}}{\sqrt{\lambda}} - \beta \right)^2 + 1 \right]^{-1/2} = \pm \sqrt{\frac{\lambda}{\mu}} \quad (\text{A.11})$$

for

$$\beta = \frac{a}{\sqrt{\lambda}}. \quad (\text{A.12})$$

Integrate (A.11) with Mathematica to obtain:

$$\tanh^{-1} \left[\frac{1 - \beta \left(\frac{\bar{p}}{\sqrt{\lambda}} - \beta \right)}{\sqrt{\beta^2 + 1} \sqrt{\left(\frac{\bar{p}}{\sqrt{\lambda}} - \beta \right)^2 + 1}} \right] = \mp \sqrt{\frac{a^2 + \lambda}{\mu}} \bar{z} + c_2. \quad (\text{A.13})$$

In order to satisfy the boundary condition at $\bar{z} = +\infty$, we must take the plus sign on the right side of (A.13). Also, (A.2) implies:

$$c_2 = \tanh^{-1} \left(\frac{a^2 - a + \lambda}{\sqrt{a^2 + \lambda} \sqrt{(a-1)^2 + \lambda}} \right). \quad (\text{A.14})$$

Equation (A.13) can be rewritten:

$$\frac{\bar{p}}{\sqrt{\lambda}} = \beta + \frac{\beta \pm (\beta^2 + 1) \tanh \omega \operatorname{sech} \omega}{\beta^2 \operatorname{sech}^2 \omega - \tanh^2 \omega}, \quad (\text{A.15})$$

with

$$\omega = L \sqrt{\frac{\beta^2 + 1}{\kappa \varepsilon_0 \varepsilon_W}} \bar{z} + c_2. \quad (\text{A.16})$$

It is straightforward to check that:

$$\lim_{\bar{z} \rightarrow \infty} \bar{p} = \lim_{\omega \rightarrow \infty} \bar{p} = 0, \quad (\text{A.17})$$

so our earlier choice of $c_1 = 0$ was correct. Now, define $\omega^* = \sinh^{-1} \beta$ and note that:

$$\beta^2 \operatorname{sech}^2 \omega^* - \tanh^2 \omega^* = 0, \quad (\text{A.18})$$

$$\tanh \omega^* \operatorname{sech} \omega^* = \frac{\beta}{\beta^2 + 1}. \quad (\text{A.19})$$

If we take the plus sign in (A.15), then $\lim_{\omega \rightarrow \omega^*} \bar{p}(\omega) = +\infty$. The solution \bar{p} should be continuous for $\omega > c_2$, and we therefore take the minus sign in (A.15) to get the solution:

$$\frac{\bar{p}}{\sqrt{\lambda}} = \beta + \frac{\beta - (\beta^2 + 1) \tanh \omega \operatorname{sech} \omega}{\beta^2 \operatorname{sech}^2 \omega - \tanh^2 \omega} = \frac{\beta^2 + 1}{\beta + \sinh \omega}. \quad (\text{A.20})$$

The dimensionless polarization $\bar{p}(\bar{z})$ depends on the phenomenological parameters λ , μ , and a . We now make several assumptions in order to estimate these parameters. First, suppose that:

$$\frac{d^2 \bar{p}}{d \bar{z}^2}(\bar{z} = 0) = 0. \quad (\text{A.21})$$

Since $\bar{p}(0) = 1$, (A.6) and (A.21) imply:

$$\lambda = (2 - a)(a - 1). \quad (\text{A.22})$$

So $\lambda < \frac{1}{4}$, and because $\lambda > 0$ by (A.9), we see that $1 < a < 2$ as well. Note that $\delta = \delta(a)$ by combining (A.9) and (A.22).

Next, observe that the quantity $\sqrt{\beta^2 + 1}$ controls the length scale of the problem through ω in (A.20). This length scale is maximized when β is minimized. Using (A.22), we can write:

$$\beta = \frac{a}{\sqrt{(2 - a)(a - 1)}}, \quad (\text{A.23})$$

which is minimized at:

$$a = \frac{4}{3}. \quad (\text{A.24})$$

Under the assumptions (A.22) and (A.24), the solution (A.15) can be written:

$$\bar{p} = \frac{3\sqrt{2}}{2\sqrt{2} + \sinh \omega}, \quad \omega = \frac{3z}{\sqrt{\varepsilon_0 \varepsilon_W \kappa}} + \tanh^{-1} \sqrt{\frac{2}{3}}. \quad (\text{A.25})$$

From (A.9) and (A.22), we also obtain the estimate:

$$\delta^2 = 1 \times 10^{-25} \text{ m}^2 \text{ N}^{-1}. \quad (\text{A.26})$$

The only phenomenological parameter left to estimate is κ . With a and λ chosen as above, (A.6) is:

$$\mu \bar{p}_{\bar{z}\bar{z}} = 2\bar{p}(\bar{p} - 1)^2. \quad (\text{A.27})$$

Observe that $\bar{p}_{\bar{z}\bar{z}} = 0$ at the boundaries $\bar{z} = 0, +\infty$. In the interior, $\bar{p}_{\bar{z}\bar{z}} > 0$ since $0 < \bar{p} < 1$. Therefore, $\bar{p}_{\bar{z}\bar{z}}$ has a maximum at some \hat{z} , $0 < \hat{z} < \infty$. In the region $\bar{z} < \hat{z}$ near the surface, the polarization is quickly decreasing from the boundary value of 1. Away from the surface, $\bar{z} > \hat{z}$, the polarization has decayed close to zero. The distance \hat{z} from the surface where $\bar{p}_{\bar{z}\bar{z}}$ is maximized therefore gives a good estimate of the width of the interfacial layer.

We will suppose that $\bar{p}_{\bar{z}\bar{z}}$ is maximized at $z = L_{\text{IF}}$, where L_{IF} is an experimental measurement of the width of the interfacial layer. Let $\omega_{\text{IF}} = \omega(\bar{z} = L_{\text{IF}}/L)$:

$$\omega_{\text{IF}} = \frac{3L_{\text{IF}}}{\sqrt{\varepsilon_0 \varepsilon_W \kappa}} + \tanh^{-1} \sqrt{\frac{2}{3}}. \quad (\text{A.28})$$

Based on the earlier discussion, we assume:

$$\frac{d^3 \bar{p}}{d \bar{z}^3} \Big|_{\bar{z}=L_{\text{IF}}/L} = 0, \quad (\text{A.29})$$

or

$$\left(\frac{\partial}{\partial \omega} \right)^3 \left(\frac{1}{2\sqrt{2} + \sinh \omega} \right) \Big|_{\omega=\omega_{\text{IF}}} = 0. \quad (\text{A.30})$$

Equation (A.30) implies:

$$\omega_{\text{IF}} = \sinh^{-1}(\sqrt{2}) \quad \text{or} \quad \omega_{\text{IF}} = \sinh^{-1}(7\sqrt{2}), \quad (\text{A.31})$$

with $\omega_{\text{IF}} = \sinh^{-1}(7\sqrt{2})$ and $\varepsilon_W = 80$, (A.28) implies:

$$\kappa = (3.7 \times 10^9 \text{ N m}^2 \text{ C}^{-2}) L_{\text{IF}}^2. \quad (\text{A.32})$$

The width of the interfacial layer can grow to almost 3 mm over the course of a few hours [3]. Using the estimate:

$$L_{\text{IF}} = 2 \text{ mm}, \quad (\text{A.33})$$

from equation (A.32) we finally estimate:

$$\kappa = 1.5 \times 10^4 \text{ N m}^4 \text{ C}^{-2}. \quad (\text{A.34})$$

Using (A.4), we find that the polarization $p(z)$ (with dimension) is:

$$p(z) = \frac{p_0 \sqrt{\lambda} (\beta^2 + 1)}{\beta + \sinh \omega}. \quad (\text{A.35})$$

The electric potential Φ in (14) can then be computed from Poisson's equation,

$$\Phi' = \frac{p}{\varepsilon_0 \varepsilon_W}, \quad (\text{A.36})$$

and the remaining boundary condition $\Phi(+\infty) = 0$.

ORCID iDs

A Earls  <https://orcid.org/0000-0003-2911-4223>
 M-C Calderer  <https://orcid.org/0000-0002-9117-7439>
 M Desroches  <https://orcid.org/0000-0002-9325-4207>
 A Zarnescu  <https://orcid.org/0000-0002-3620-6196>
 S Rodrigues  <https://orcid.org/0000-0002-3601-5760>

References

[1] Chai B, Yoo H and Pollack G H 2009 Effect of radiant energy on near-surface water *J. Phys. Chem. B* **113** 13953–8

[2] Zheng J-M, Wexler A and Pollack G H 2009 Effect of buffers on aqueous solute-exclusion zones around ion-exchange resins *J. Colloid Interface Sci.* **332** 511–4

[3] Florea D, Musa S, Huyghe J M R and Wyss H M 2014 Long-range repulsion of colloids driven by ion exchange and diffusiophoresis *Proc. Natl Acad. Sci.* **111** 6554–9

[4] Zheng J-M, Chin W-C, Khijniak E, Khijniak E and Pollack G H 2006 Surfaces and interfacial water: evidence that hydrophilic surfaces have long-range impact *Adv. Colloid Interface Sci.* **127** 19–27

[5] Chai B, Mahtani A G and Pollack G H 2012 Unexpected presence of solute-free zones at metal-water interfaces *Contemp. Mater.* **3** 1

[6] Ball P 2008 Water as an active constituent in cell biology *Chem. Rev.* **108** 74–108

[7] Chaplin M F 2001 Water: its importance to life *Biochem. Mol. Biol. Educ.* **29** 54–59

[8] Schurr J M 2013 Phenomena associated with gel–water interfaces. analyses and alternatives to the long-range ordered water hypothesis *J. Phys. Chem. B* **117** 7653–74

[9] Esplandiu M J, Reguera D and Fraxedas J 2020 Electrophoretic origin of long-range repulsion of colloids near water/nafion interfaces *Soft Matter* **16** 3717–26

[10] Elton D C, Spencer P D, Riches J D and Williams E D 2020 Exclusion zone phenomena in water—a critical review of experimental findings and theories *Int. J. Mol. Sci.* **21** 5041

[11] Pollack G H 2013 *The Fourth Phase of Water: Beyond Solid, Liquid and Vapor* (Seattle, WA: Ebner and Sons Publishers)

[12] Fumagalli L *et al* 2018 Anomalously low dielectric constant of confined water *Science* **360** 1339–42

[13] Chen C-S, Chung W-J, Hsu I C, Wu C-M and Chin W-C 2012 Force field measurements within the exclusion zone of water *J. Biol. Phys.* **38** 113–20

[14] Huszár I N, Mártonfalvi Z, Laki A J, Iván K and Kellermayer M 2014 Exclusion-zone dynamics explored with microfluidics and optical tweezers *Entropy* **16** 4322–37

[15] Jabs H and Rubik B 2014 Self-organization at aqueous colloid-membrane interfaces and an optical method to measure the kinetics of exclusion zone formation *Entropy* **16** 5954–75

[16] Matyushov D V 2021 Dielectric susceptibility of water in the interface *J. Phys. Chem. B* **125** 8282–93

[17] Liu X *et al* 2021 Nonthermal and reversible control of neuronal signaling and behavior by midinfrared stimulation *Proc. Natl Acad. Sci.* **118** e2015685118